

Article

Thermal Performance Improvement for Different Strategies of Battery Thermal Management Systems Combined with Jute—A Comparison Study †

Rekabra Youssef ^{1,2,*}, Md Sazzad Hosen ¹, Jiacheng He ¹, Mohammed AL-Saadi ^{1,2}, Joeri Van Mierlo ¹ and Maitane Berecibar ¹

¹ Mobility, Logistics & Automotive Technology Research Group (MOBI), Electrical Engineering and Energy Technology (ETEC) Department, Vrije Universiteit Brussel, 1050 Brussels, Belgium; md.sazzad.hosen@vub.be (M.S.H.); jiacheng.he@vub.be (J.H.); Mohammed.al-saadi@vub.be (M.A.-S.); Joeri.Van.Mierlo@vub.be (J.V.M.); Maitane.Berecibar@vub.be (M.B.)

² Flanders Make, 3001 Heverlee, Belgium

* Correspondence: Rekabra.Youssef@vub.be

† This article is a revised version of our paper published in 2021 IEEE the 9th International Conference on Smart Grid and Clean Energy Technologies (ICSGCE), Sarawak, Malaysia, 15–17 October 2021, pp. 68–71.

Abstract: Jute is a cheap, eco-friendly, widely available material well-known for its cooling properties. In electric vehicles (EVs), dissipating a huge amount of the heat generated from lithium-ion batteries with an efficient, light, and low-power consumption battery thermal management system (BTMS) is required. In our previous study, jute fibers were proposed and investigated as a novel medium to enhance the cooling efficiency of air-based battery thermal management systems. In this paper, as the first attempt, jute was integrated with a phase change material (PCM) passive cooling system, and the thermal performance of a 50 Ah prismatic battery was studied. Temperature evolution, uniformity, and cooling efficiency were investigated. A comparison between the thermal behavior of the air-based BTMS and PCM-assisted cooling system was performed. The results indicated that adding jute to the BTMS increased the cooling efficiency and especially decreased the temperature development. Furthermore, the temperature difference (ΔT) efficiency was enhanced by 60% when integrating jute with PCM, and temperature uniformity improved by 3% when integrating jute with air-based BTMS. This article compared the integration of jute with active cooling and passive cooling; thus, it shed light on the importance of jute as a novel, eco-friendly, lightweight, cheap, available, and nontoxic material added to two strategies of BTMS. The setup was physically made and experimentally studied for the purpose of BTMS optimization.

Keywords: jute; electric vehicles; thermal management; evaporative cooling; passive cooling; air cooling; phase change material (PCM); lithium-ion battery



Citation: Youssef, R.; Hosen, M.S.; He, J.; AL-Saadi, M.; Van Mierlo, J.; Berecibar, M. Thermal Performance Improvement for Different Strategies of Battery Thermal Management Systems Combined with Jute—A Comparison Study †. *Energies* **2022**, *15*, 873. <https://doi.org/10.3390/en15030873>

Academic Editors: Alon Kuperman and Alessandro Lampasi

Received: 17 November 2021

Accepted: 18 January 2022

Published: 25 January 2022

Publisher's Note: MDPI stays neutral with regard to jurisdictional claims in published maps and institutional affiliations.



Copyright: © 2022 by the authors. Licensee MDPI, Basel, Switzerland. This article is an open access article distributed under the terms and conditions of the Creative Commons Attribution (CC BY) license (<https://creativecommons.org/licenses/by/4.0/>).

1. Introduction

The electric vehicle (EV) market has matured over the last few decades because of the future it promises of environmental and green transportation with zero emissions [1]. The lithium-ion battery (LIB) is the most preferred energy storage system used by the majority of EVs [2] because of their large energy, high cycle life, light weight, and low rate of self-discharge [3]. On the other hand, the performance characteristics of LIBs are strongly limited by their operating temperature [4,5]. High charge and discharge produce a huge amount of heat [6] and nonuniform surface temperature distribution [6,7]. Moreover, heat generation can diminish battery performance [8,9], leading to a quick thermal runaway [10]. Therefore, solutions to this issue are demanded to exceed the last stage of large-energy LIB applications. Maintaining the operating temperature within the proper range requires an effective battery thermal management system (BTMS) [11]. As

pointed out by many researchers [12], BTMSs can be classified into air cooling (active and passive cooling) [13], liquid cooling [14], phase change material (PCM) cooling [15], heat pipe cooling [16], and hybrid cooling [17], which is a combination of two or more of the mentioned cooling strategies.

A liquid cooling system is the most common cooling strategy used in electrified vehicles [18]. Because of high thermal conductivity and heat transfer efficiency [19], it can control battery temperature development and distribution [20]. However, liquid cooling systems have complexity in structure, water leakage risk, and additional weight and energy consumption [21].

The heat pipe has better thermal performance and higher thermal conductivity [22] compared to the other passive cooling strategies, but the contact area of the heat pipe system with the battery is small, and the system structure is volumetric [23,24].

Air cooling systems are considered one of the most traditional, common, and widely embraced cooling strategies in industrial applications [25]. This is due to their simplicity in structure, flexibility in maintenance and packaging, water leakage avoidance, and low weight and power consumption [26]. However, the main concerning points are low cooling efficiency and nonuniform temperature distribution [27]. Nevertheless, respectable research efforts have been employed to optimize the air cooling strategy [28]. Na et al. [29] proposed an optimization for an air cooling BTMS with a reverse airflow design. They compared the results with unidirectional airflow by computational fluid dynamics (CFD) and declared that the maximum average temperature differences were enhanced with a reverse airflow design. Chen et al. [30] improved the BTMS with U-type airflow and concluded that battery temperature difference and power consumption were minimized. Wang et al. [31] experimentally found that by reciprocating airflow, uneven temperature distribution caused by heat accumulation could be mitigated. Xie et al. [32] experimentally and numerically researched the effects of inlet and outlet angles and the channel width between battery cells on the heat dissipation rate. They revealed that airflow channels had a remarkable influence on the maximum temperature rise and the temperature difference. In terms of safety, alternative BTMSs have been studied and proposed, such as helium-based [33] and ammonia-based [34] battery thermal management.

A phase change material (PCM) is a substance that can absorb or release heat at a specific temperature value when it reaches the melting point and transforms from one physical phase to another [35,36]. The PCM absorbs the heat accumulated on the battery surface by conduction [37]. It has large latent heat and constitutes a low-cost thermal management strategy [38]. On the other hand, PCMs suffer from low thermal conductivity, and thermal management systems based on them are considered volumetric and massive. Therefore, many studies have been recorded to overcome these disadvantages [39]. Hussain et al. [40] used paraffin as a phase change material and infiltrated it into graphene-coated nickel foam. They claimed that the battery temperature rise was decreased by 17%. Li et al. [41] proposed an optimized design to reduce the mass and volume of PCMs. Huo et al. [42] employed a porous medium for PCM heat transfer improvement. Zhang et al. [43] suggested a combination of PCMs and designed a composite of olin/expanded graphite (EG)/paraffin. They found that the complex could control the battery temperature rise at 45 °C ambient conditions and a high discharge rate.

A respectable research effort has been performed to optimize battery thermal management either experimentally [42,43] or by thermal modeling [44,45].

All the mentioned studies were carried out targeting battery thermal management system optimization. Most of the optimization techniques did not take environmental aspects into consideration and even ignored them at some stages. Moreover, leakage, bulkiness, volumetric, uneven temperature distribution, and complexity in design are the most common issues between all existing battery thermal management systems. Therefore, in this paper, environmental and novel design optimization is proposed to enhance battery thermal management performance and design. Jute, as a cheap, eco-friendly, lightweight, available, and novel cooling medium, was integrated as a first attempt into a BTMS [46]. An

active air cooling strategy was chosen as the common BTMS used in industrial applications. Then, jute was integrated into the system, and the results indicated an improvement in battery thermal performance [46].

In this study, a promising passive cooling strategy, a PCM with high latent heat, was chosen to combine with jute, since the PCM strategy is not enough to maintain the temperature within the preferable scope, especially for the demands of future EVs with fast charging. Therefore, merging further cooling mediums such as jute with PCM was hypothesized to contribute to enhancing thermal performance and lowering the temperature increase.

Therefore, the PCM cooling strategy was built with and without jute. Then, the thermal behavior of a 50 Ah prismatic battery cell was investigated. Maximum temperature, temperature differences, and distribution with cooling efficiency were analyzed. A comparison among different BTMSs (natural convection, active air cooling, and passive PCM cooling) integrated with jute was studied. The results indicated that integrating jute with BTMSs improved thermal performance with less weight, cost, and equipment, with respect of the environmental side, and kept the main purpose of EVs within the environmental aspect. The remainder of the paper is arranged as follows: Section 2 describes the experimental setup and the proposed design, Section 3 discusses and analyzes the thermal performance of integrating jute with PCM, and Section 4 presents the analysis for integrating jute with air-based BTMS. A comparison among BTMSs integrated with jute is represented in Section 5 and the experimental uncertainty analysis is given in Section 6. Finally, the conclusion and future work are drawn in Section 7.

2. Methodology and Development

A prismatic lithium-ion battery holding a large capacity of 50 Ah was used; its specifications are reported in Table 1.

Table 1. Battery properties declared by the manufacture.

Item	Parameter Specification
Nominal capacity	50 Ah
Nominal voltage	3.7 V
Battery weight	900 ± 25 g
Battery dimension	148 × 98 × 27 mm

With the aim of generating as much heat as possible, a high, constant current of 125 A (meaning a 2.5 °C discharge rate) was injected into the battery, first in natural convection without any cooling system. Then, jute fibers were prepared to be integrated into the following cooling strategies: active air cooling using fans and passive cooling with PCM assistance. Afterward, battery temperature increase, temperature distribution, and cooling efficiency were investigated for each of the cooling strategies integrated with jute. In the end, a comparison between the proposed BTMSs was made. Figure 1 gives an overview of the experiments carried out and result analysis.

2.1. Experimental Setup

In order to conduct trustworthy and accurate tests, an experimental test bench was built in the MOBI (mobility, logistics, and automotive technology research center) laboratory at Vrije Universiteit Brussel. The equipment and setup used in this study can be divided into general setup and specific setup.

The specific setup is illustrated and clarified separately in the following section for each cooling strategy. However, the general test bench and setup is shown in Figure 2. It consisted of a battery tester (PEC manufactured ACT0550 model) with an accuracy of ±0.005% for the voltage reading, used to cycle the battery; a CTS manufactured climate chamber, to control battery surface temperature; four thermocouples with accuracy of ±3%, used for temperature measurements; and a microcontroller device, used to record the thermocouples' temperature readings. Finally, all the mentioned equipment were linked

to a computer to monitor the parameters (voltage, current, and temperature) and acquire the data.

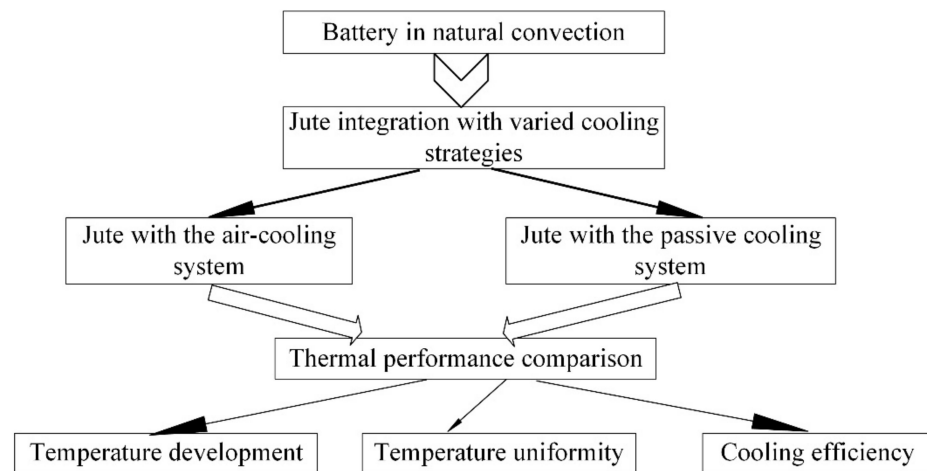


Figure 1. Design of the study and work flowchart.

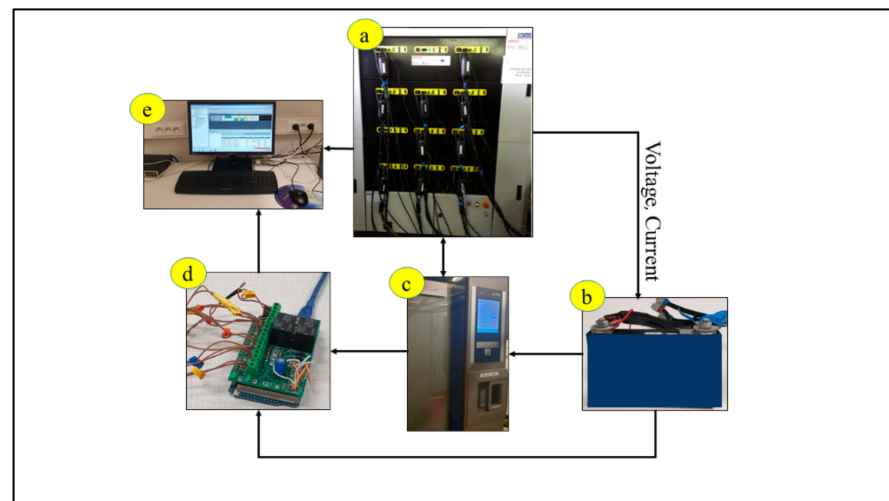


Figure 2. Schematic of the test bench: (a) battery tester; (b) 50 Ah battery; (c) climate chamber; (d) microcontroller; (e) computer.

2.2. Description of the Proposed Designs

Jute is considered a low-cost, natural fiber [47] and cellulosic material [48]. Because of its attractive cooling efficiency, light weight, low cost, and environmental benefits [49–51], it was chosen to insert into a battery thermal management system. Dedicated test setups were designed and constructed to evaluate the performance of jute fibers used in two strategies of BTMS, which are described in the following subsections.

2.2.1. Passive Cooling PCM-Assisted BTMS

An illustrative image of the proposed design as it was tested in this study is shown in Figure 3. Four thermocouples (glass-encapsulated sensors, standard type, B57560G, B57560G1) with accuracy of $\pm 3\%$ were used for temperature measurement. Three thermocouples were attached to the front side of the battery at the locations shown in Figure 3, and the fourth was used to record the ambient temperature. Then, the battery was surrounded with jute mesh and placed in a plexiglass case constructed to fit with the battery, jute, PCM, and thermocouples. A composite paraffin/graphite PCM was prepared, representing the passive cooling system. Its thermophysical properties are given in Table 2.

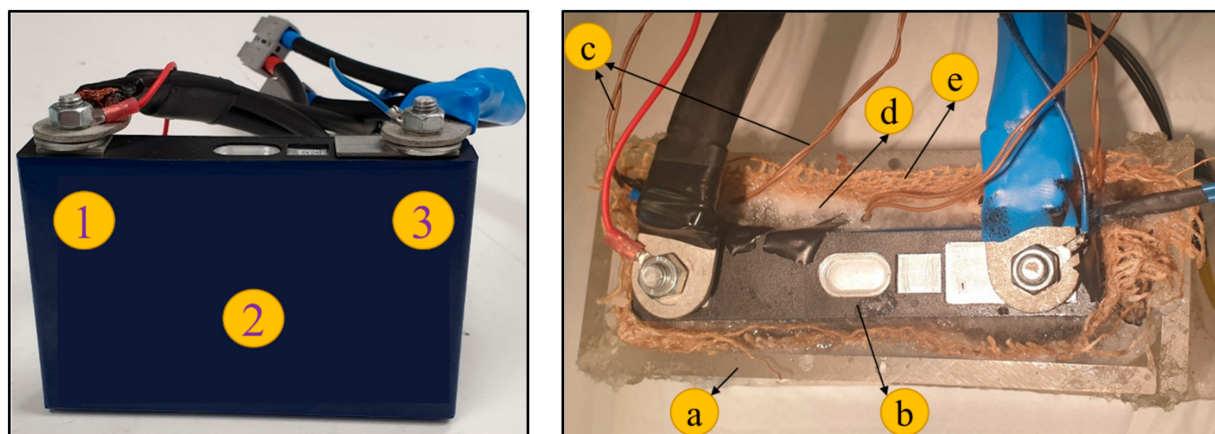


Figure 3. Thermocouple locations on the battery surface (left); PCM case with jute (right): (a) plexiglass case; (b) battery; (c) thermocouples; (d) PCM; (e) jute.

Table 2. Specifications and thermophysical properties for the PCM used.

Properties	Value
Thermal conductivity	2.32 W/m·K
Heat capacity	1430 J/kg·K
Density	1305 kg/m ³
Melting temperature	27–28 °C
Latent heat	150,000 J/kg

The PCM complex was poured into the plexiglass casing at an environmental temperature of 25 °C. The battery was discharged from a 100% state of charge (SoC) to a 0% state of charge, and the temperature was recorded at three cooling conditions. First, battery temperature measurements were taken inside the case without any PCM or jute. Then, PCM was poured into the case, and the measurement was recorded in the presence of the paraffin/graphite PCM. Finally, jute was wrapped around the battery periphery and PCM was poured into the plastic casing.

2.2.2. Active Air Cooling BTMS

An illustrative image of the test bench for air cooling with jute is shown in Figure 4. A casing was prototyped from plexiglass, and the battery was placed in cross-section inside the casing. Four fans were set on both sides of the case. Two fans on one side were used to blow the air with a speed of 7 m/s, and air circulation surrounded the battery before exiting from the suction fans with airflow of 2.5 m/s on the opposite side of the case.

A frame of jute fibers was prepared to fit with the case side. Furthermore, a filling water system was designed to feed the jute with water and drain the extra water from the cooling system.

For the purpose of validating the proposed air-based cooling design, a high discharge current (125 A) was applied to the battery with four conditions of airflow for the proposed design. The first condition featured two functional suction fans while the opposite side fans were in off mode and not operated. In the second condition, the air cooling case was operated with four fans; two fans were used as inlets, and the airflow traveled through the case to the other two suction fans (outlets). Then, the jute frame with the water filling system was fixed to the cooling case, replacing the inlet fans, in the third condition. In this condition, the jute was saturated with water and revealed to the exhaust fans, where the airflow evaporated the water from the jute's surface and cooled down the battery temperature. Therefore, the jute was wet at the beginning of the test and was then dehydrated. In the fourth condition, the jute frame was kept in its place, facing the suction fans, but it was refilled with water and maintained as wet during the entire test time.

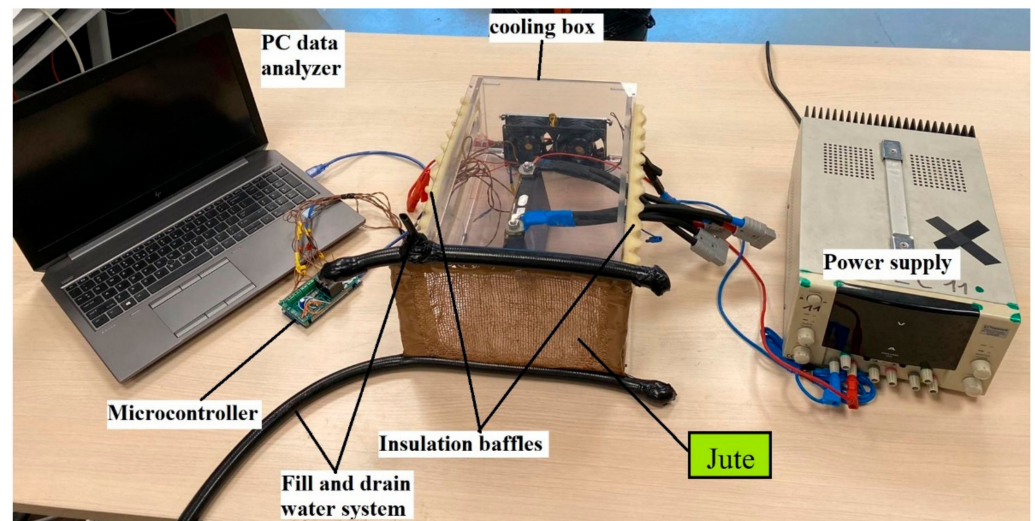


Figure 4. Proposed air cooling design with jute (Reprinted with permission from ref. [46]).

3. Thermal Performance of Jute Integration with PCM-Assisted Cooling System

The amount of thermal energy that could be stored in the jute fabric increased by applying PCMs on its textiles. This was due to the nature of PCMs and latent heat. When the battery was wrapped with jute fabric integrated with PCMs, the battery grew cooler when its temperature rose and hotter when the battery temperature decreased. This was because the heat from the battery was used to melt the PCMs in the jute fabric, essentially cooling the battery down. Furthermore, when the battery temperature decreased again, the energy stored as latent heat was released again, which in turn kept the battery warmer for a longer duration.

3.1. Temperature Development

Temperature development (evolution) and increase were calculated as the average surface temperature among the three thermocouples attached to the battery. Figure 5 compares the temperature increase in three tests, which were performed to represent the cases of no cooling (Box), cooling assisted with PCM, and cooling with jute merged into PCM. As expected, the use of PCM resulted a noteworthy reduction in the surface temperature. The maximum temperature for the battery surface reaches 46 °C in the no-cooling condition, but applying the PCM as a cooling medium decreased the maximum temperature at the end of discharge to 40 °C. Furthermore, an additional reduction in temperature occurred when jute was merged with PCM; a maximum temperature of 36 °C was obtained when the battery was fully discharged. This was because the thermal properties and cooling efficiency of jute were enhanced by merging it with the PCM [51–53], which led to better cooling performance.

3.2. Uniformity

Temperature uniformity can be defined as the temperature distribution throughout the cell surface. This distribution becomes more nonuniform at critical discharge current, which leads to heat accumulation and thermal runaway [52,53]. To measure the cooling uniformity for the proposed cooling strategy, the temperature nonuniformity (temperature distribution) over the surface of the battery was analyzed in this research. It was studied as the average of the differences between every two contiguous points of temperature obtained at the three thermal sensor locations. Figure 6 shows the temperature nonuniformity (temperature distribution) versus time for all three cases studied. The maximum nonuniformity of the temperature distribution on the battery surface was 2.7 °C, 2.4 °C, and 7.14 °C for the no-cooling (box), PCM cooling, and PCM+jute conditions, respectively. The pure PCM cooling case achieved the best temperature uniformity, whereas the PCM+jute response

of heat dissipation was slower, and the temperature distribution was mostly nonuniform. The deficiency in thermal performance could have been due to the fiber cumulation and the absence of uniformity in the distribution the of jute [51–55].

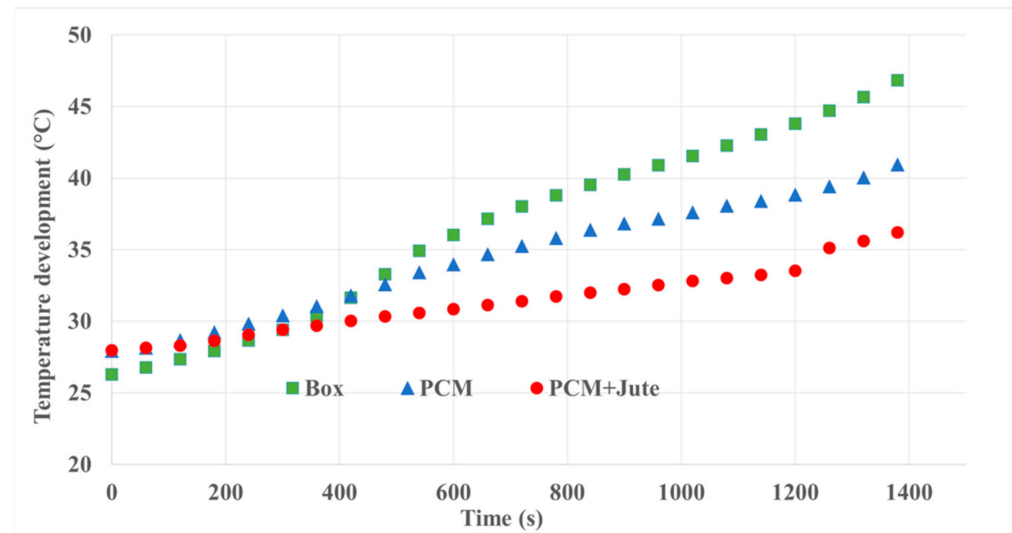


Figure 5. Temperature increase over time during fast discharge with a constant high current of 125 A.

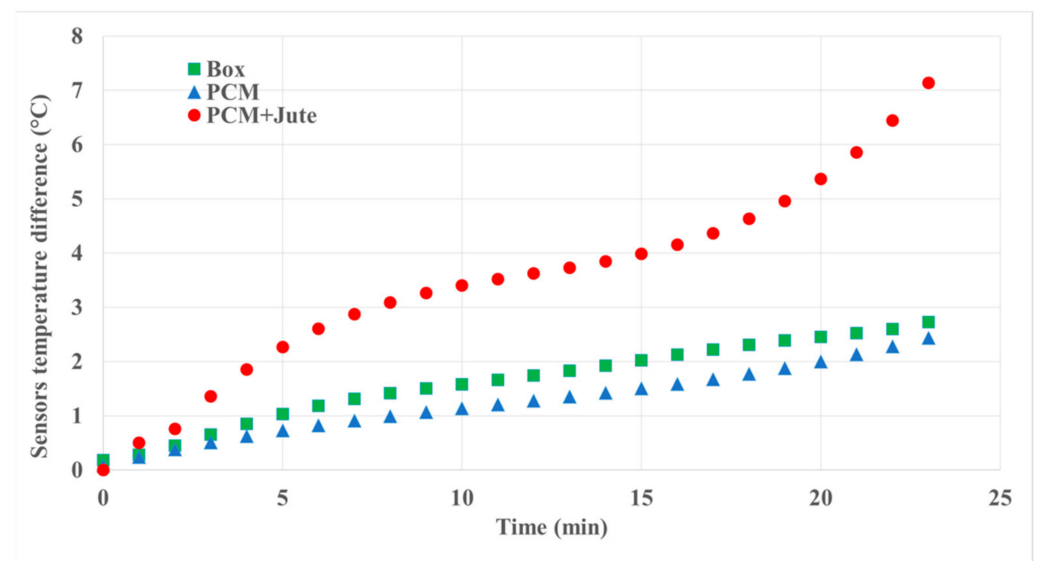


Figure 6. Temperature nonuniformity (temperature distribution) as a function of time for the passive cooling strategy.

3.3. Efficiency

Three parameters were considered to determine the cooling efficiency: maximum temperature (T_{max}) efficiency, temperature increase (ΔT) efficiency, and uniformity efficiency. The maximum temperature for every cooling scenario, $T_{max(k)}$, was compared with the maximum temperature that the battery reached without any cooling system, $T_{max(Box)}$ (Equation (1)). The same was done for battery uniformity efficiency (Equation (2)). Then, because the initial temperature for the three cases did not have an equal value, it was trustworthy to give a comparison of delta T for both cooling cases. Delta T (ΔT) represents the difference between the maximum temperature the battery reached and the initial tem-

perature at every time interval. Then, ΔT efficiency was calculated the same way as T_{max} efficiency and uniformity efficiency (Equation (3)).

$$T_{max}\text{efficiency} = \frac{T_{max(\text{Box})} - T_{max(k)}}{T_{max(\text{Box})}} \times 100 \quad (1)$$

$$T_{max}\text{efficiency} = \frac{T_{max(\text{Box})} - T_{max(k)}}{T_{max(\text{Box})}} \times 100 \quad (2)$$

$$\Delta T \text{ efficiency} = \frac{\Delta T_{max(\text{Box})} - \Delta T_{max(k)}}{\Delta T_{max(\text{Box})}} \times 100 \quad (3)$$

The efficiency comparison between the PCM cooling strategy and the PCM+jute cooling technique is clarified in Figure 7. Uniformity efficiency was not achieved with the PCM+jute technique. However, the maximum temperature efficiency was enhanced with the PCM+jute technique by 23%, which indicated better performance than the PCM cooling strategy (13% T_{max} efficiency). Moreover, a notable improvement in ΔT efficiency occurred when jute was embedded in the PCM. Increases in ΔT efficiency of 37% and 60% were obtained for the PCM and PCM+jute cooling strategies, respectively.

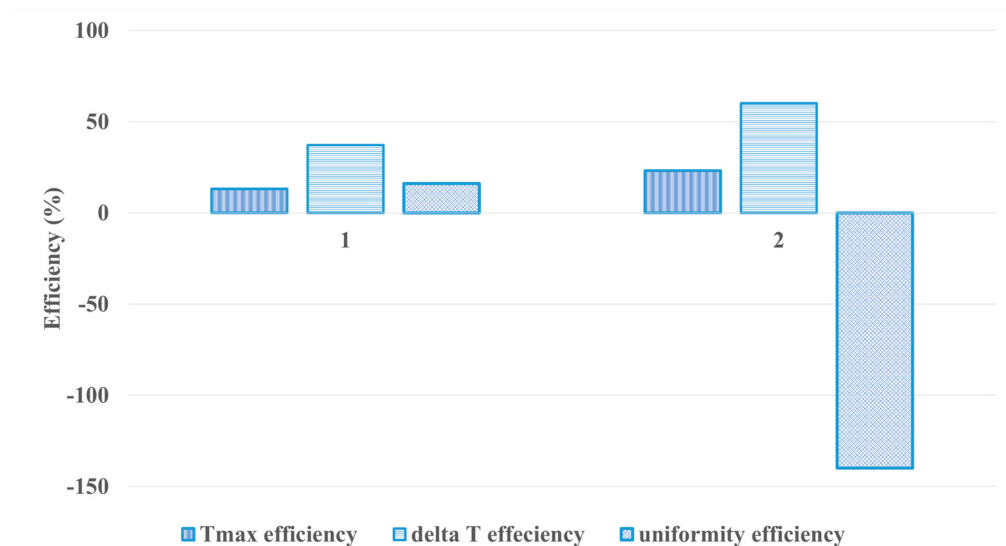


Figure 7. Efficiency comparison for cooling strategies: (1) PCM, (2) PCM+jute.

4. Thermal Performance of Jute Integration with Air Cooling Strategy

When moistened jute fabric is affected by a hot environment, the latent heat is absorbed by some of the water droplets, which then evaporate and change their phase from liquid to vapor [53]. Moreover, the remaining nonabsorbed water withdraws from the jute fabric to the outside air.

4.1. Temperature Development (Evolution)

Temperature development and increase were calculated as the average of the temperatures recorded at the three thermocouple locations. The average temperature trend is plotted in Figure 8, which displays the curves of average surface temperatures for the battery cell over time for the following cooling five cases: no-cooling (NC) condition; a forced air cooling strategy including two cases, first with two outflow fans and second with both inflow and inflow fans; then combining air cooling with jute for evaporative cooling; and the fourth cooling case evaporative cooling through entirely wet jute. The most aggressive temperature rise was recorded for the case of no cooling (NC), in which the temperature reached 48 °C when the battery fully discharged. Then, the temperature was diminished impressively by the case of using two exhaust fans, reaching approximately 40.5 °C. A

significant reduction in temperature occurred in the evaporative cooling case, where jute was integrated into the forced cooling. With this integration, an interesting improvement in the cooling was obtained during the discharge process of about two degrees on average. This was due to the vacuum position of the jute, where it enhanced and cooled down the airflow temperature. Although jute helped with cooling, air humidity contributed to a further increase in temperature, and this was noticed with both cases of integrating jute (wet until getting dehydrated and wet throughout the discharge time). However, the final temperature reached with evaporative cooling was about 38.5 °C. Nonetheless, with the use of four fans, the highest temperature obtained was around 37.5 °C, which was the lowest maximum temperature that occurred among all the forced cooling cases. This discussion resulted in a novel outcome, that the same rate of cooling improvement occurred by using four fans or two fans. However, by utilizing jute, further reduction in weight, power consumption, and cost can be gained.

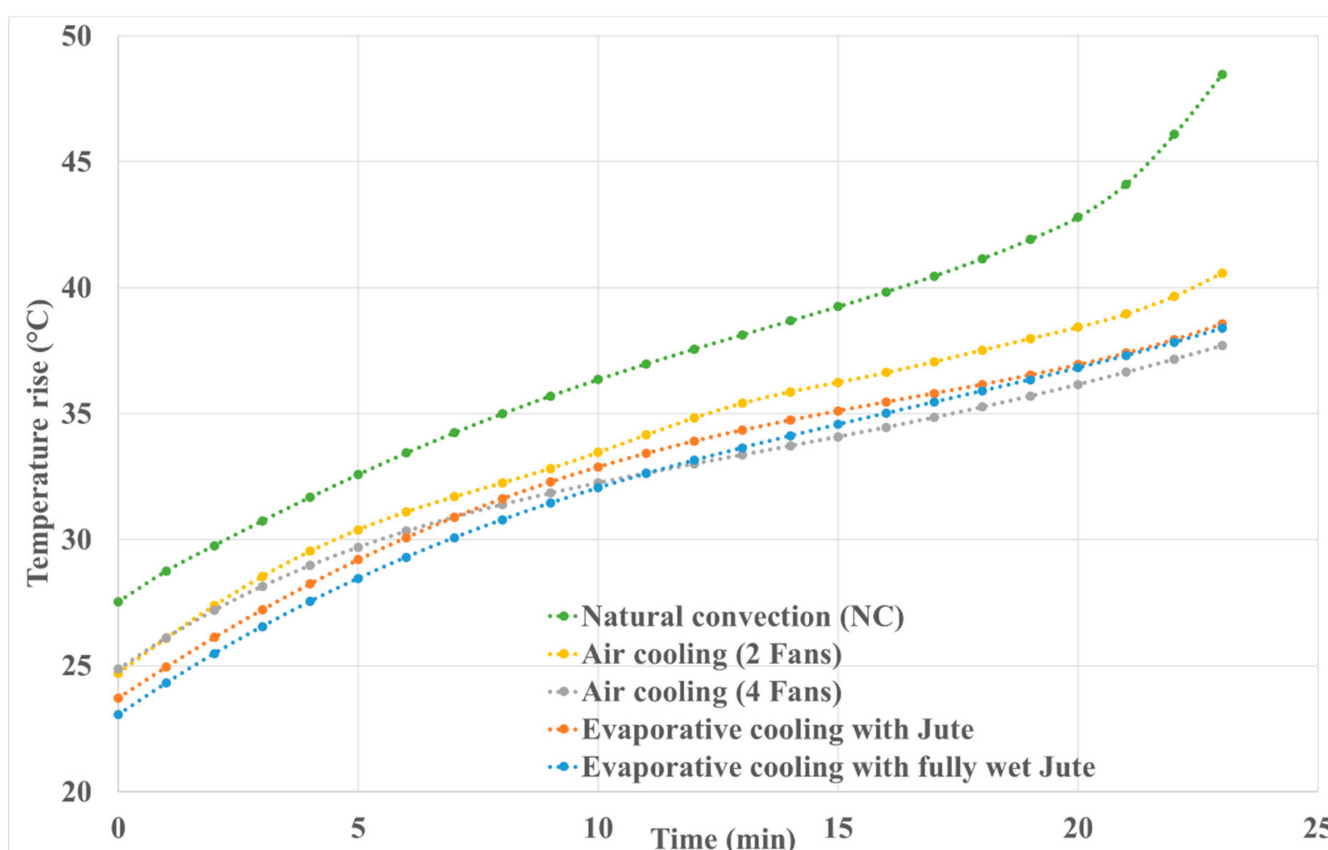


Figure 8. Battery surface temperature as a function of time for all the tests (Reprinted with permission from ref. [46]).

4.2. Uniformity

The temperature nonuniformity (distribution) over the battery surface was studied and calculated the same way as described in Section 3.2. Figure 9 shows the nonuniformity temperature versus time for all active cooling strategies. Each second, the measurement was recorded twice; therefore, the horizontal axis represents the time field and is the discharge time duplicated. It was found that except for evaporative cooling with fully wet jute, the temperature uniformity for all cooling strategies increased progressively to meet the peak when the battery was completely discharged. The maximum nonuniformity on the battery surface was 1.29 °C, 1.42 °C, 1.40 °C, and 1.39 °C for the natural air convection with no cooling (NC), air cooling with two fans, air cooling with four fans, and evaporative cooling with jute, respectively. However, in the fully wet jute cooling scenario, the uniformity characteristic grew at the early part of the battery discharge process, then arrived at a mostly

stationary status and kept semi steady uniformity characteristics between 0.5 and 1 °C. Furthermore, close to the highest temperature, the temperature distribution for evaporative cooling with the fully wet jute strategy was the lowest among the active cooling strategies.

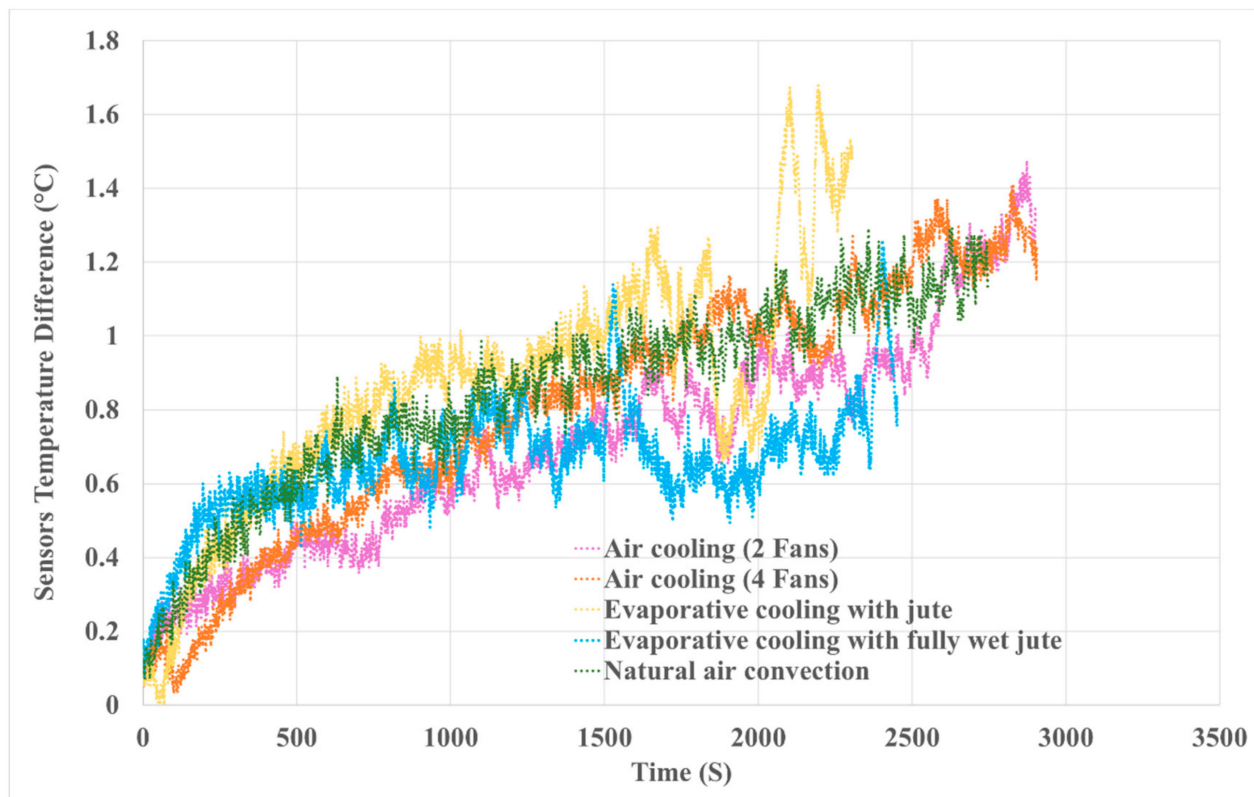


Figure 9. The nonuniformity temperature distribution versus time for different air-based cooling strategies (Reprinted with permission from ref. [46]).

4.3. Efficiency

All the active cooling strategies' efficiencies, in terms of maximum temperature (T_{max}) efficiency, temperature increase (ΔT) efficiency, and uniformity efficiency, are summarized in Figure 10. T_{max} , ΔT , and uniformity efficiency were calculated the same way as explained in Section 3.3. The T_{max} efficiency for all active cooling strategies fluctuated between 14% and 20%. The best cooling system in terms of T_{max} efficiency was the cooling scenario with four fans; in second place, the cooling scenario with jute achieved an efficiency of 18.7%. Furthermore, ΔT efficiency reached 44.45% with the four-fan cooling strategy and 33.06% with the wet jute strategy. Uniformity efficiency was accomplished exclusively in the wet jute strategy by 2.5%. Last but not the least, it is noteworthy that integrating wet jute with an active cooling strategy could contribute to improving the cooling efficiency in terms of T_{max} , ΔT , and uniformity simultaneously.

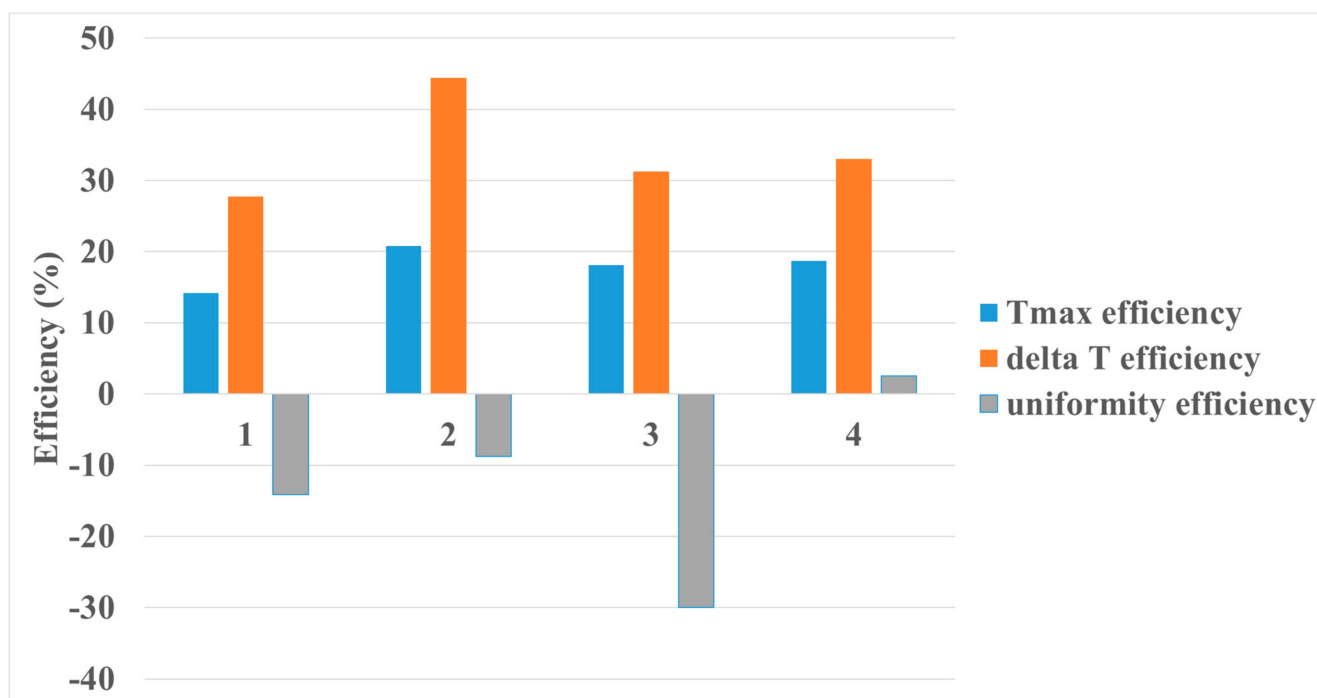


Figure 10. Efficiency comparison for cooling strategies: (1) air cooling (two suction fans); (2) air cooling (suction and blow fans); (3) evaporative cooling with jute; (4) evaporative cooling with fully wet jute (Reprinted with permission from ref. [46]).

5. Thermal Performance Comparison of Combining Jute into the (Active Cooling) Air-Based Cooling Strategy and (Passive Cooling) PCM-Assisted Cooling Strategy

5.1. Temperature Development

Figure 11 compares the changes in the average battery surface temperatures measured by thermocouples under different cooling conditions. The thermal schematic shows that the battery temperature reached the highest value, around 48 °C, in natural air convection with no cooling (NC). The temperature increment decreased by applying different cooling strategies: cooling with fans (active cooling), evaporative cooling (EC) with combined jute, and passive cooling assisted with PCM. Comparing active cooling and EC, EC with wet jute obtained a relatively close result to active cooling with four fans, but with less equipment, weight, and power consumption. Moreover, comparing EC with passive cooling, an additional reduction in temperature occurred with passive cooling integrated with jute. It can be concluded that jute had a positive impact on both environmental aspects and temperature enhancement for cooling strategy optimization.

5.2. Uniformity

According to Figure 12, the use of the PCM+jute technique decreased the temperature uniformity more than the rest of the cooling strategies. However, with the use of jute integrated into the active cooling with fans, the uniformity was enhanced, and an improvement in temperature distribution was achieved.

5.3. Efficiency

In Figure 13, all the performed characterizations are abbreviated to a single plot, which describes and compares the efficiency for every cooling scenario. Maximum temperature (T_{max}) and ΔT efficiency were generally achieved under most of the cooling strategies, but integrating jute with PCM led to the highest T_{max} and ΔT efficiency at 23% and 60%, respectively. Uniformity efficiency was not accomplished under most of the cooling strategies, excepting PCM and EC with wet jute. Therefore, it can be concluded that jute had a

remarkable impact on the cooling efficiency in terms of T_{max} , ΔT , and uniformity and could be integrated into BTMS design optimization.

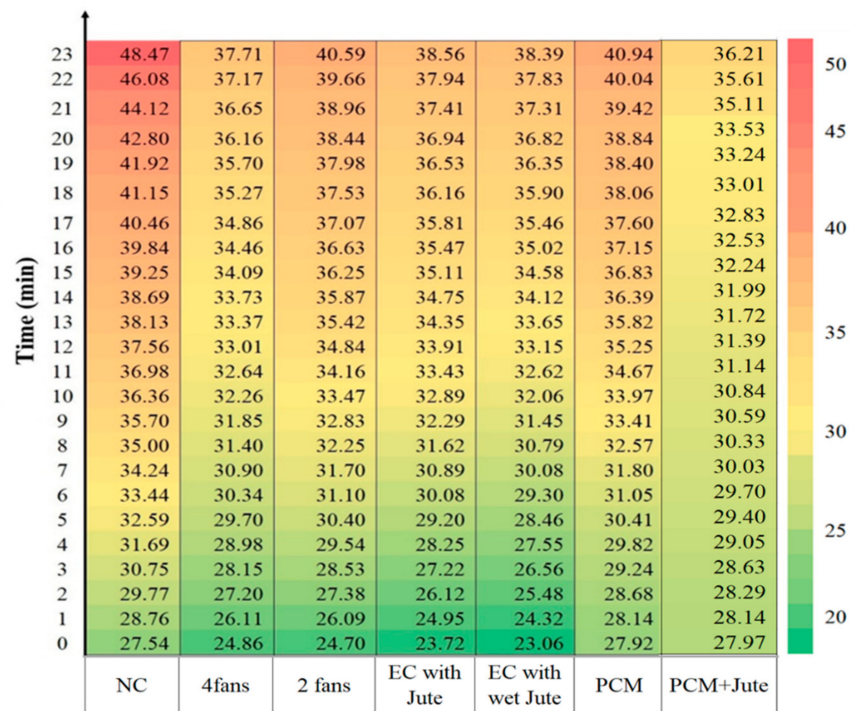


Figure 11. Comparison of the average surface temperature rise for all the discussed cooling strategies.

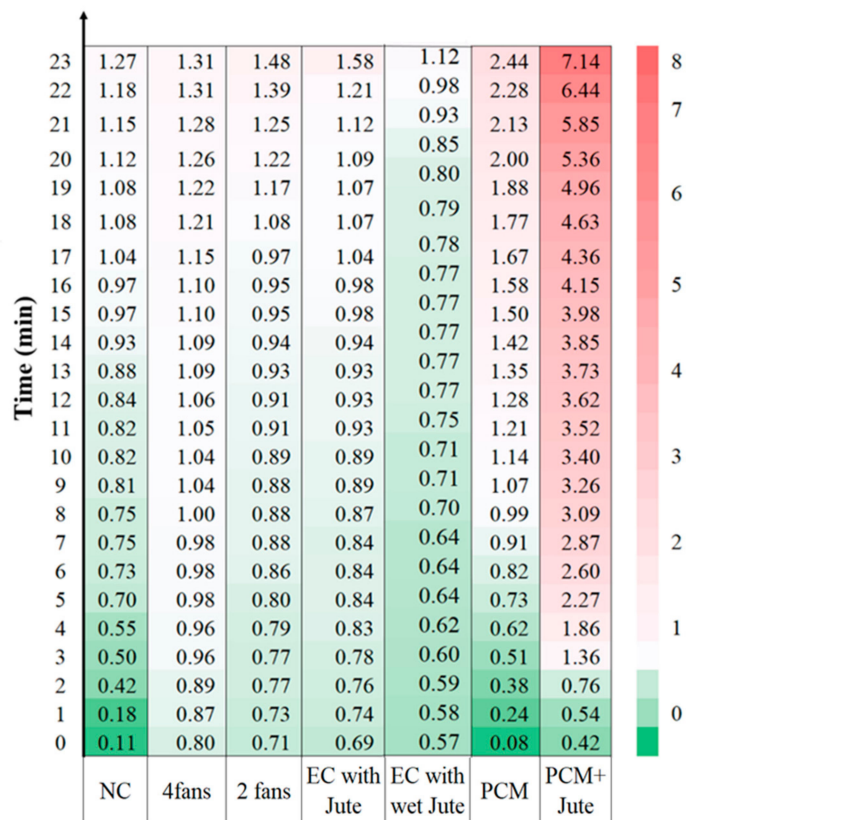


Figure 12. Comparison of nonuniformity temperature distributions for all the discussed cooling strategies.



Figure 13. Efficiency comparison for cooling strategies: (1) PCM, (2) PCM+jute, (3) 2 fans, (4) 4 fans, (5) EC with jute, (6) EC with wet jute.

6. Experimental Uncertainty Analysis

Using the method presented by Moffat [56], the experiment error analysis was estimated.

Assuming that the result, S , of the experiment is acquired from a set of measurements as follows:

$$S = S(x_1, x_2, x_3, \dots, x_n)$$

The uncertainty is specified by the following equation:

$$\delta S = \left\{ \sum_{k=1}^n \left(\frac{\partial R}{\partial x_k} \delta x_k \right)^2 \right\}^{1/2} \quad (4)$$

where δS is the total uncertainty and δx_k is the uncertainty of every singular measurement. The uncertainties of experimental equipment were assumed as the absolute bias given by the aperture specification and described in Section 2.1. However, the uncertainty of the average temperature measurement was acquired based on the average temperature of the thermocouples attached to the cell. Thus, the total uncertainties were calculated following Equation (5) and estimated as 3.6%.

$$\frac{\Delta T_R}{T_R} = \sqrt{\sum_{i=1}^4 (\Delta T_{Ri} / T_{Ri})^2} \quad (5)$$

7. Conclusion and Future Work

This study attempted to investigate and analyze a novel and environmental optimization for LIB thermal management systems by integrating jute fiber with an active cooling strategy and a passive cooling strategy with PCM. It concluded with interesting results, which are summarized as follows:

1. Integrating jute fabrics with PCM (passive cooling strategy) achieved the desired effect on the battery thermal behavior and enhanced the cooling efficiency; temperature difference (ΔT) efficiency was enhanced by 60%. Furthermore, less PCM and

nonenvironmental cooling material was used. Therefore, system weight reduction and environmental material enhancement were achieved.

2. By adding jute to active cooling, high cooling efficiency was delivered with the wet jute in terms of maximal temperature, ΔT , and temperature uniformity; the latter improved by 3%. Merging jute into BTMS design would boost the opportunities for electric vehicles to work properly in hot environments.
3. Comparing the integration of jute with active cooling (air-based) and passive cooling (PCM), the results indicated that uniformity efficiency with the PCM+jute technique was mostly not achieved, while it was enhanced with the active cooling strategy. Therefore, integrating jute into an active BTMS has great potential to improve BTMS cooling efficiency in terms of T_{max} , ΔT , and uniformity together.
4. Last but certainly not least, jute, as a novel, eco-friendly, weightless, cheap, available, and nontoxic material, was added to two strategies of BTMS. The setup was physically made and experimentally studied for the purpose of BTMS design optimization. This work will be extended in the future to the modeling stage and simulation. Jute fabric thermal properties will be studied more, and further investigation with analysis will be added to optimize battery thermal management environmentally.

Author Contributions: Conceptualization, Methodology, Software, Validation, Formal analysis, Investigation, Resources, Data Curation, Writing—Original Draft, Visualization, and Writing—Review & Editing, R.Y.; Writing—Review & Editing, M.S.H.; Writing—Review & Editing, J.H.; Supervision & Project administration, M.A.-S.; Supervision & Project administration, J.V.M.; Supervision & Project administration, M.B. All authors have read and agreed to the published version of the manuscript.

Funding: European Union Horizon 2020 research and innovation program under Grant Agreement No. 824311, the study was mainly developed within the framework of the ACHILES project.

Institutional Review Board Statement: Not applicable.

Informed Consent Statement: Not applicable.

Data Availability Statement: Not applicable.

Acknowledgments: This study was mainly developed within the framework of the ACHILES project, which has received the funding from the European Union Horizon 2020 research and innovation program under Grant Agreement No. 824311. The authors also wish to acknowledge Flanders Make for support to the MOBI research group.

Conflicts of Interest: The authors declare no conflict of interest.

References

1. Muratori, M.; Alexander, M.; Arent, D.; Bazilian, M.; Cazzola, P.; Dede, E.M.; Farrell, J.; Gearhart, C.; Greene, D.; Jenn, A.; et al. The rise of electric vehicles—2020 status and future expectations. *Prog. Energy* **2021**, *3*, 022002. [[CrossRef](#)]
2. Sanguesa, J.; Torres-Sanz, V.; Garrido, P.; Martinez, F.; Marquez-Barja, J. A Review on Electric Vehicles: Technologies and Challenges. *Smart Cities* **2021**, *4*, 372–404. [[CrossRef](#)]
3. Yoshio, M.; Brodd, R.J.; Kozawa, A. *Lithium-Ion Batteries*; Springer: Berlin/Heidelberg, Germany, 2009.
4. Bandhauer, T.M.; Garimella, S.; Fuller, T.F. A Critical Review of Thermal Issues in Lithium-Ion Batteries. *J. Electrochem. Soc.* **2011**, *158*, R1. [[CrossRef](#)]
5. He, J.; Youssef, R.; Hosen, S.; Akbarzadeh, M.; Van Mierlo, J.; Bercebar, M. A novel methodology to determine the specific heat capacity of lithium-ion batteries. *J. Power Sources* **2021**, *520*, 230869. [[CrossRef](#)]
6. Youssef, R.; Hosen, S.; He, J.; Jaguemont, J.; Akbarzadeh, M.; De Sutter, L.; Van Mierlo, J.; Bercebar, M. Experimental and Numerical Study on the Thermal Behavior of a Large Lithium-Ion Prismatic Cell With Natural Air Convection. *IEEE Trans. Ind. Appl.* **2021**, *57*, 6475–6482. [[CrossRef](#)]
7. Lin, J.; Liu, X.; Li, S.; Zhang, C.; Yang, S. A review on recent progress, challenges and perspective of battery thermal management system. *Int. J. Heat Mass Transf.* **2021**, *167*, 120834. [[CrossRef](#)]
8. Ma, S.; Jiang, M.; Tao, P.; Song, C.; Wu, J.; Wang, J.; Deng, T.; Shang, W. Temperature effect and thermal impact in lithium-ion batteries: A review. *Prog. Nat. Sci.* **2018**, *28*, 653–666. [[CrossRef](#)]
9. Youssef, R.; He, J.; Akbarzadeh, M.; Jaguemont, J.; De Sutter, L.; Bercebar, M.; Van Mierlo, J. Investigation of Thermal Behavior of Large Lithium-Ion Prismatic Cell in Natural Air Convection. In Proceedings of the 2020 9th International Conference on Renewable Energy Research and Application (ICRERA), Glasgow, UK, 27–30 September 2020; pp. 43–47. [[CrossRef](#)]

10. Feng, X.; Ren, D.; He, X.; Ouyang, M. Mitigating Thermal Runaway of Lithium-Ion Batteries. *Joule* **2020**, *4*, 743–770. [[CrossRef](#)]
11. Kim, J.; Oh, J.; Lee, H. Review on battery thermal management system for electric vehicles. *Appl. Therm. Eng.* **2019**, *149*, 192–212. [[CrossRef](#)]
12. Jaguemont, J.; Van Mierlo, J. A comprehensive review of future thermal management systems for battery-electrified vehicles. *J. Energy Storage* **2020**, *31*, 101551. [[CrossRef](#)]
13. Zhang, X.; Li, Z.; Luo, L.; Fan, Y.; Du, Z. A review on thermal management of lithium-ion batteries for electric vehicles. *Energy* **2022**, *238*, 121652. [[CrossRef](#)]
14. Thakur, A.K.; Prabakaran, R.; Elkadeem, M.; Sharshir, S.W.; Arıcı, M.; Wang, C.; Zhao, W.; Hwang, J.-Y.; Saidur, R. A state of art review and future viewpoint on advance cooling techniques for Lithium-ion battery system of electric vehicles. *J. Energy Storage* **2020**, *32*, 101771. [[CrossRef](#)]
15. Liu, C.; Xu, D.; Weng, J.; Zhou, S.; Li, W.; Wan, Y.; Jiang, S.; Zhou, D.; Wang, J.; Huang, Q. Phase Change Materials Application in Battery Thermal Management System: A Review. *Materials* **2020**, *13*, 4622. [[CrossRef](#)] [[PubMed](#)]
16. Zhang, Z.; Wei, K. Experimental and numerical study of a passive thermal management system using flat heat pipes for lithium-ion batteries. *Appl. Therm. Eng.* **2020**, *166*. [[CrossRef](#)]
17. Kong, D.; Peng, R.; Ping, P.; Du, J.; Chen, G.; Wen, J. A novel battery thermal management system coupling with PCM and optimized controllable liquid cooling for different ambient temperatures. *Energy Convers. Manag.* **2020**, *204*, 112280. [[CrossRef](#)]
18. Liu, H.; Wei, Z.; He, W.; Zhao, J. Thermal issues about Li-ion batteries and recent progress in battery thermal management systems: A review. *Energy Convers. Manag.* **2017**, *150*, 304–330. [[CrossRef](#)]
19. Yang, W.; Zhou, F.; Zhou, H.; Wang, Q.; Kong, J. Thermal performance of cylindrical lithium-ion battery thermal management system integrated with mini-channel liquid cooling and air cooling. *Appl. Therm. Eng.* **2020**, *175*, 115331. [[CrossRef](#)]
20. Deng, Y.; Feng, C.; Jiaqiang, E.; Zhu, H.; Chen, J.; Wen, M.; Yin, H. Effects of different coolants and cooling strategies on the cooling performance of the power lithium ion battery system: A review. *Appl. Therm. Eng.* **2018**, *142*, 10–29. [[CrossRef](#)]
21. Xia, G.; Cao, L.; Bi, G. A review on battery thermal management in electric vehicle application. *J. Power Sources* **2017**, *367*, 90–105. [[CrossRef](#)]
22. Yang, X.; Yan, Y.Y.; Mullen, D. Recent developments of lightweight, high performance heat pipes. *Appl. Therm. Eng.* **2012**, *33*, 1–14. [[CrossRef](#)]
23. Zou, H.; Wang, W.; Zhang, G.; Qin, F.; Tian, C.; Yan, Y. Experimental investigation on an integrated thermal management system with heat pipe heat exchanger for electric vehicle. *Energy Convers. Manag.* **2016**, *118*, 88–95. [[CrossRef](#)]
24. Wang, Q.; Jiang, B.; Xue, Q.; Sun, H.; Li, B.; Zou, H.; Yan, Y. Experimental investigation on EV battery cooling and heating by heat pipes. *Appl. Therm. Eng.* **2015**, *88*, 54–60. [[CrossRef](#)]
25. Volkswagen E-Up! Air Cooled Battery, Featured in ViaVision Magazine | My Electric Car Forums n.d. Available online: <https://www.myelectriccarforums.com/volkswagen-e-up-air-cooled-battery-featured-in-viavision-magazine/> (accessed on 17 June 2021).
26. Zhao, G.; Wang, X.; Negnevitsky, M.; Zhang, H. A review of air-cooling battery thermal management systems for electric and hybrid electric vehicles. *J. Power Sources* **2021**, *501*, 230001. [[CrossRef](#)]
27. Numerical Investigation of Thermal Behaviors in Lithium-Ion Battery Stack Discharge | Elsevier Enhanced Reader n.d. Available online: <https://reader.elsevier.com/reader/sd/pii/S0306261914007053?token=28CCD1C09F370C552B30C563E03D4360789A389587DCD03455AF641EB4997591FB5E9493D6F3F3F6629A58C1933B719B&originRegion=eu-west-1&originCreation=20210623085040> (accessed on 23 June 2021).
28. Akinlabi, A.H.; Solyali, D. Configuration, design, and optimization of air-cooled battery thermal management system for electric vehicles: A review. *Renew. Sustain. Energy Rev.* **2020**, *125*, 109815. [[CrossRef](#)]
29. Na, X.; Kang, H.; Wang, T.; Wang, Y. Reverse layered air flow for Li-ion battery thermal management. *Appl. Therm. Eng.* **2018**, *143*, 257–262. [[CrossRef](#)]
30. Chen, K.; Song, M.; Wei, W.; Wang, S. Structure optimization of parallel air-cooled battery thermal management system with U-type flow for cooling efficiency improvement. *Energy* **2018**, *145*, 603–613. [[CrossRef](#)]
31. Wang, S.; Li, K.; Tian, Y.; Wang, J.; Wu, Y.; Ji, S. Improved thermal performance of a large laminated lithium-ion power battery by reciprocating air flow. *Appl. Therm. Eng.* **2019**, *152*, 445–454. [[CrossRef](#)]
32. Xie, J.; Ge, Z.; Zang, M.; Wang, S. Structural optimization of lithium-ion battery pack with forced air cooling system. *Appl. Therm. Eng.* **2017**, *126*, 583–593. [[CrossRef](#)]
33. Alipour, M.; Hassanpouryouzband, A.; Kizilel, R. Investigation of the Applicability of Helium-Based Cooling System for Li-Ion Batteries. *Electrochem* **2021**, *2*, 135–148. [[CrossRef](#)]
34. Al-Zareer, M.; Dincer, I.; Rosen, M.A. Electrochemical modeling and performance evaluation of a new ammonia-based battery thermal management system for electric and hybrid electric vehicles. *Electrochimica Acta* **2017**, *247*, 171–182. [[CrossRef](#)]
35. Siddique, A.R.M.; Mahmud, S.; Van Heyst, B. A comprehensive review on a passive (phase change materials) and an active (thermoelectric cooler) battery thermal management system and their limitations. *J. Power Sources* **2018**, *401*, 224–237. [[CrossRef](#)]
36. Souayfane, F.; Fardoun, F.; Biwole, P.-H. Phase change materials (PCM) for cooling applications in buildings: A review. *Energy Build.* **2016**, *129*, 396–431. [[CrossRef](#)]
37. Landini, S.; Leworthy, J.; O'donovan, T. A Review of Phase Change Materials for the Thermal Management and Isothermalisation of Lithium-Ion Cells. *J. Energy Storage* **2019**, *25*. [[CrossRef](#)]

38. Bose, P.; Amirtham, V.A. A review on thermal conductivity enhancement of paraffinwax as latent heat energy storage material. *Renew. Sustain. Energy Rev.* **2016**, *65*, 81–100. [[CrossRef](#)]
39. Verma, A.; Shashidhara, S.; Rakshit, D. A comparative study on battery thermal management using phase change material (PCM). *Therm. Sci. Eng. Prog.* **2019**, *11*, 74–83. [[CrossRef](#)]
40. Hussain, A.; Abidi, I.H.; Tso, C.Y.; Chan, K.; Luo, Z.; Chao, C.Y. Thermal management of lithium ion batteries using graphene coated nickel foam saturated with phase change materials. *Int. J. Therm. Sci.* **2018**, *124*, 23–35. [[CrossRef](#)]
41. Li, Y.; Du, Y.; Xu, T.; Wu, H.; Zhou, X.; Ling, Z.; Zhang, Z. Optimization of thermal management system for Li-ion batteries using phase change material. *Appl. Therm. Eng.* **2018**, *131*, 766–778. [[CrossRef](#)]
42. Lyu, P.; Huo, Y.; Qu, Z.; Rao, Z. Investigation on the thermal behavior of Ni-rich NMC lithium ion battery for energy storage. *Appl. Therm. Eng.* **2020**, *166*, 114749. [[CrossRef](#)]
43. Zhang, X.; Liu, C.; Rao, Z. Experimental investigation on thermal management performance of electric vehicle power battery using composite phase change material. *J. Clean. Prod.* **2018**, *201*, 916–924. [[CrossRef](#)]
44. Li, Y.; Wei, Z.; Xiong, B.; Vilathgamuwa, D.M. Adaptive Ensemble-Based Electrochemical-Thermal-Degradation State Estimation of Lithium-ion Batteries. *IEEE Trans. Ind. Electron.* **2021**, *1*. [[CrossRef](#)]
45. Wu, J.; Wei, Z.; Liu, K.; Quan, Z.; Li, Y. Battery-Involved Energy Management for Hybrid Electric Bus Based on Expert-Assistance Deep Deterministic Policy Gradient Algorithm. *IEEE Trans. Veh. Technol.* **2020**, *69*, 12786–12796. [[CrossRef](#)]
46. Youssef, R.; Hosen, S.; He, J.; Jaguemont, J.; De Sutter, L.; Van Mierlo, J.; Bercibar, M. Effect analysis on performance enhancement of a novel and environmental evaporative cooling system for lithium-ion battery applications. *J. Energy Storage* **2021**, *37*, 102475. [[CrossRef](#)]
47. Shah, S.S.; Shaikh, M.N.; Khan, M.Y.; Alfasane, A.; Rahman, M.M.; Aziz, A. Present Status and Future Prospects of Jute in Nanotechnology: A Review. *Chem. Rec.* **2021**, *21*, 1631–1665. [[CrossRef](#)]
48. Chattopadhyay, D.; Patel, B.H.; Chattopadhyay, D.P.; Patel, B.H. Imparting water repellency to jute fabric by nano paraffin and nano copper colloid treatment Functional finishing of textiles with natural resources. View project Imparting water repellency to jute fabric by nano paraffin and nano copper colloid treatment. n.d. Available online: <https://www.researchgate.net/publication/308334126> (accessed on 15 November 2021).
49. Jahan, A. The environmental and economic prospects of jute with a connection to social factors for achieving Sustainable Development. Independent Master thesis Advanced level, Uppsala University, Uppsala, Sweden, 2019.
50. El Nemr, A. From natural to synthetic fibers. In *Textiles: Types, Uses and Production Methods*; Nova Science Publishers, Inc.: Hauppauge, NY, USA, 2012.
51. Brend, D.E.C.; Eva, B.; Ignacio, M.; Pablo, D.; Jaime, G.; Valérie, D.E.V. Structural influence on the thermal behavior of jute fabrics treated with pcms. n.d. pp. 43–46. Available online: <http://textile.webhost.uoradea.ro/Annals/Vol%20XIX-No%201-2018/Textile/Art.%20no.%20290-pag.%2043-46.pdf> (accessed on 20 January 2022).
52. Al-Sulaiman, F. Evaluation of the performance of local fibers in evaporative cooling. *Energy Convers. Manag.* **2002**, *43*, 2267–2273. [[CrossRef](#)]
53. Feng, X.; Ouyang, M.; Liu, X.; Lu, L.; Xia, Y.; He, X. Thermal runaway mechanism of lithium ion battery for electric vehicles: A review. *Energy Storage Mater.* **2018**, *10*, 246–267. [[CrossRef](#)]
54. Babapoor, A.; Azizi, M.; Karimi, G. Thermal management of a Li-ion battery using carbon fiber-PCM composites. *Appl. Therm. Eng.* **2015**, *82*, 281–290. [[CrossRef](#)]
55. Yuen, M.; Chen, L. Heat-transfer measurements of evaporating liquid droplets. *Int. J. Heat Mass Transf.* **1978**, *21*, 537–542. [[CrossRef](#)]
56. Moffat, R.J. Describing the uncertainties in experimental results. *Exp. Therm. Fluid Sci.* **1988**, *1*, 3–17. [[CrossRef](#)]